PROTEINS
STRUCTURE ■ FUNCTION ■ BIOINFORMATICS

Exploring the free energy landscape of a model β-hairpin peptide and its isoform

Chitra Narayanan* and Cristiano L. Dias*

Department of Physics, New Jersey Institute of Technology, University Heights, Newark, New Jersey 07102-1982

ABSTRACT

Secondary structural transitions from α-helix to β-sheet conformations are observed in several misfolding diseases including Alzheimer's and Parkinson's. Determining factors contributing favorably to the formation of each of these secondary structures is therefore essential to better understand these disease states. β-hairpin peptides form basic components of antiparallel β-sheets and are suitable model systems for characterizing the fundamental forces stabilizing β-sheets in fibrillar structures. In this study, we explore the free energy landscape of the model β-hairpin peptide GB1 and its E2 isoform that preferentially adopts α-helical conformations at ambient conditions. Umbrella sampling simulations using all-atom models and explicit solvent are performed over a large range of end-to-end distances. Our results show the strong preference of GB1 and the E2 isoform for β-hairpin and α-helical conformations, respectively, consistent with previous studies. We show that the unfolded states of GB1 are largely populated by misfolded β-hairpin structures which differ from each other in the position of the β-turn. We discuss the energetic factors contributing favorably to the formation of α-helix and β-hairpin conformations in these peptides and highlight the energetic role of hydrogen bonds and non-bonded interactions.

Proteins 2014; 00:000–000.

Key words: potential of mean force; GB1; misfolded β-hairpin; hydrogen bonding; reptation.

INTRODUCTION

Proteins fold into specific conformations, dictated by their amino acid sequence, resulting in unique functions. A variety of human diseases such as Alzheimer's, Parkinson's, and type II diabetes are associated with the incorrect folding of amyloid proteins.[1,2] These misfolded protein structures aggregate into fibrils exhibiting a high content of β-strands arranged into parallel[3–9] or antiparallel[10–15] orientations. Thus, protein misfolding can involve the structural reorganization from coil and/or α-helical conformations to β-strands under denaturing conditions[16,17] and disease states.[8,18,19] A variety of factors including point mutations,[20–22] changes in pH,[23] and partially denaturing conditions[24] have been shown to influence the rate of α-helix to β-sheet transition.

Experiments suggest that association of misfolded proteins into fibrils occurs for all amino acid sequences under appropriate denaturing conditions, implying that fibril structures emerge from properties that are common to all proteins, that is, the backbone.[1] In this scenario, the role of side chain interactions is to modulate the propensity for fibril formation. Accordingly, experiments have shown that increasing the hydrophobicity of nucleating regions[25,26] and the presence of aromatic residues[27] increases the propensity of fibril formation. Moreover, hydrophobic interactions favored the formation of β-sheet structures[28–30] and they penalized α-helical conformations in model peptides.[29,30] This could rationalize why some amyloid peptides form preferentially β or coil structures in aqueous environments and α-helical conformations in membrane mimicking environments.[31–33] In contrast to hydrophobic interactions, mutations increasing the net charge of peptides inhibit fibril formation.[34] Computer simulations have also explored pathways for the inter-conversion of α-helix to β-sheet. This interconversion occurs either through a random coil intermediate[35] or through a zipping mechanism.[36]

β-Hairpin peptides are suitable model systems for characterizing the fundamental forces stabilizing

Additional Supporting Information may be found in the online version of this article.

*Correspondence to: Cristiano L. Dias, Department of Physics, New Jersey Institute of Technology, Newark, NJ 07102. E-mail: cld@njit.edu or Chitra Narayanan, Department of Physics, New Jersey Institute of Technology, Newark, NJ 07102. E-mail: chtra@njit.edu

Received 26 September 2013; Revised 21 March 2014; Accepted 29 April 2014
Published online 13 May 2014 in Wiley Online Library (wileyonlinelibrary.com).
DOI: 10.1002/prot.24601

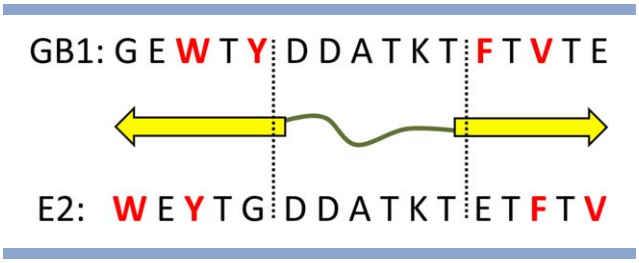

Figure 1

Primary sequence of GB1 and the E2 isoform and a schematic representation of the secondary structure corresponding to GB1. Hydrophobic residues are indicated in red. [Color figure can be viewed in the online issue, which is available at wileyonlinelibrary.com.]

β-sheets. In particular, GB1 peptide (GEWTYDDATKTFTVTE), the C-terminal β-hairpin region (residues 41–56) of protein G, is amenable to computational studies[37–48] due to its small size, stability of its β-hairpin conformation, and fast folding kinetics (∼6 μs).[26,38] Garcia and Sanbonmatsu[37] first showed using replica exchange simulations in explicit water that GB1 has a small propensity for α-helical conformations, in addition to the predominant β-hairpin conformation. The α-helical conformations were also observed in subsequent studies of the peptide in implicit solvent.[38,49] Levy and coworkers[49] calculated the free energy difference between the α-helical and β-hairpin states to be 1.573 ± 0.018 kcal/mol. They showed that the transition from α-helix to β-hairpin conformations begins with the association of the hydrophobic core even before the formation of native hydrogen bonds. Hence, changing the position of non-polar residues within the amino acid sequence is expected to affect the formation of the hydrophobic core and the stability of α and β conformers.[50–52] In an interesting study, Ma and Nussinov[40] designed the E2 isoform of GB1 (WEYTGDDATKTETFTV) by moving the hydrophobic residues to the termini (see Fig. 1). Sequence-based structure prediction suggests that both peptides adopt β-hairpin conformation (see Supporting Information Fig. S1); however, Nussinov *et al.* showed that the energy landscape of the E2 isoform strongly favors helical conformations. This is remarkable as hydrophobic contacts in both peptides involve same residue pairs W–V and Y–F, and they have identical turn sequence (Fig. 1). It is an indication that β-sheet structures in GB1 are not formed solely by hydrophobic collapse or turn propensity but perhaps through a combination of both factors.[53]

In this study, we use all-atom simulations in explicit water to explore the free energy landscapes of GB1 and the E2 isoform. To this effect, we use umbrella sampling[54] with harmonic restraints applied to the ends of the chains to sample folded and unfolded conformations of the peptides. We find that the global minimum of the free energy for GB1 can be mapped to β-hairpin conformations whereas its unfolded state is populated with misfolded hairpins differing from each other in the location of the β-turn. In contrast, the energy landscape of the E2 isoform is characterized by a large presence of helical conformations. We show that an increase in peptide–peptide and water–water hydrogen bonds is observed during the formation of these structures. However, this increase is compensated by a decrease in peptide–water hydrogen bonds resulting in an insignificant change in the net number of hydrogen bonds within the explored range of end-to-end distances. These results suggest that hydrogen bonds are not main interactions driving the formation of α-helical and β-hairpin secondary structures, supported by the unfavorable electrostatic energy observed for the formation of these structures.

SIMULATION METHODOLOGY

Initial structures were prepared from amino acid sequences of GB1 (GEWTYDDATKTFTVTE) and the E2 isoform[40] (WEYTGDDATKTETFTV). Simulated annealing was performed on the extended conformations to create random structures of the peptides. Structures with the least number of hydrogen bonds were chosen from the simulated annealing step to avoid any bias of the starting conformation on the final structures.

We performed molecular dynamics simulations of the uncapped peptides at 310 K using GROMACS (GROningen MAchine Chemical Simulations, version 4.5.4)[55] simulation package and the AMBER ff99sb-ILDN[56–58] force field. Periodic boundary conditions were applied in all directions. To explore the α-helical and β-hairpin conformations of GB1 and the E2 isoform, we used the pull code in GROMACS[55] to simulate the peptides over a range of end-to-end distances between 0.3 and 2.4 nm at 0.1 nm intervals. An additional simulation was performed at 0.45 nm, which corresponds to the end-to-end distance at which a perfect β-hairpin is observed. For each simulation, the end-to-end distance was restrained to a specific value within the above-mentioned range. A force constant of 25 kcal/mol/Å^2 was used for the pull simulations. β-Hairpin conformations are expected at lower end-to-end distances (∼0.5 nm) while α-helical conformations are expected at larger end-to-end distances (∼2.2 nm).

Peptides were immersed in a 4.5 nm × 4.5 nm × 4.5 nm solvent box containing 2892 and 3623 TIP3P[59] water molecules for the GB1 and E2 isoform, respectively. Three Na^+ ions were added to neutralize the system. Protein and non-protein atoms were coupled to their respective temperature baths and maintained at 310 K. Temperature and pressure were maintained CONSTANT using the v-rescale thermostat[60] and Parrinello-Rahman barostat,[61] respectively. Simulations were performed using a 2 fs timestep. Electrostatic interactions were calculated using the Particle-Mesh Ewald approach with a

grid spacing of 0.12 nm. Electrostatic cut-off of 1.3 nm and van der Waals cut-off of 1.2 nm were used. Two sets of independent simulations were performed over the specified end-to-end distance range corresponding to a total of 23 simulations for each set. Each of the end-to-end distance simulations was performed for 400 ns. We used the last 300 ns of each of the two independent sets of simulations over the entire end-to-end range of distances. Potential of mean force (PMF) was calculated as a function of the end-to-end distance using the weighted histogram analysis method (WHAM)[62] using g_wham[63] implemented in GROMACS.

Secondary structures were calculated using the DSSP algorithm[64] which determines hydrogen bonds using an electrostatic model. In Figure 2(A,B), a strand refers to either a parallel or an anti-parallel bridge while a helix refers to α-helix, 3_{10} helix, or π-helix. For the hydrogen bond analysis in Figure 2(E,F), we used a common used geometrical definition common geometry in which hydrogen bonds are formed when the distance between donor (D) and acceptor (A) is smaller than 0.35 nm and the angle A–D–H is smaller than 40°. We used g_hbond provided in the software package GROMACS for this calculation.

Representative conformations shown in Figure 2(A,B) were selected by clustering simulation ensembles. Clustering was performed using the gromos clustering method provided with the g_cluster utility of GROMACS.[65] Further details are provided in supporting Information. In Figure 2(E–H), rescaled values of hydrogen bonds and energetic terms (van der Waals, Coulomb, and total) were calculated as the difference of these quantities at each end-to-end distance and that at 2.4 nm. Plots of the actual means for these parameters (without rescaling) are presented in Supporting Information Figures S3 and S4.

RESULTS AND DISCUSSION

Free energy landscape of GB1 and the E2 isoform shows distinct preferences for β-hairpin and α-helical conformations

The free energy landscape of GB1 and the E2 isoform is computed along the reaction coordinate corresponding to the peptide end-to-end distance in the range of 0.3–2.4 nm. Figure 2(A,B) shows the PMFs for the GB1 peptide and the E2 isoform at 310 K. Qualitative agreement is observed between the minima in the PMF and the secondary structural propensities of the peptides [Fig. 2(C,D)]. Global minimum of the free energy for GB1 is observed at end-to-end distances of 0.5 nm and it is characterized by structures with β-hairpin conformations. β-Hairpin propensity is prominent over an extended range of end-to-end distances from 0.4 to 1.6 nm [Fig. 2(C)]. Representative conformations corresponding to the different minima are shown in Figure 2(A). GB1 adopts a significant amount (∼20%) of completely folded helical conformations at larger end-to-end distances (∼2.4 nm). However, these conformations are not energetically favored. The free energy difference between the β-hairpin and α-helical conformations of GB1 is calculated to be ∼1.56 kcal/mol, consistent with that reported by Levy and coworkers.[49]

The free energy landscape of the E2 isoform is drastically different from that of the GB1 peptide. The global minimum of the free energy is observed at intermediate end-to-end-distances between 1.1 and 1.8 nm. These regions of free energy minima correspond to structures with partially folded α-helical conformations [Fig. 2(D)]. Although this peptide has a small propensity for β-hairpin conformations, these structures are not energetically favorable. This strong preference of the E2 isoform for helical conformations is consistent with observations of Ma and Nussinov.[40] Further, completely folded helical structures (observed at $\xi > 2.0$ nm) are less favorable compared to partially folded ($1.2 \text{ nm} < \xi < 1.8$ nm) helices. Partially folded helical conformations have also been observed in numerous helix stability and denaturation studies of helical peptides and proteins.[35,66–68]

Misfolded β-hairpin conformations of GB1

In the zipper-like mechanism for β-hairpin formation, native turn contacts form first followed by hydrogen bonds which zip the two strands together all the way to the N- and C-termini. During zipping, the position of the turn does not move as the end-to-end distance of the peptide decreases [Fig. 3(A)]. This symmetry is clearly not observed in our simulations of GB1 as can be seen from the characteristic configurations shown in Figure 2(A). We observe three misfolded β-hairpin conformations of GB1 differing from each other in the position of the turn. One of these conformations with non-native turn close to the N-terminus [similar to the represented structure at 1.6 nm in Fig. 2(A)] was observed previously using all-atom simulations in explicit water.[69] Furthermore, it was shown that the presence of this misfolded β-hairpin is consistent with the two state folding kinetics of GB1.[69] To the best of our knowledge, this is the first time that the other two misfolded β-hairpins shown in Figure 2(A) are reported.

In the misfolded β-hairpins, the turn is displaced from the N-terminus towards the middle of the chain with decreasing end-to-end distance, as shown in Figure 4. For large end-to-end distances ($\xi = 1.6$ nm), turns can be found anywhere from the middle of the sequence to the C-terminus. As the end-to-end distance decreases, the turn becomes more localized closer to its native position (residues 7–10). The free energy landscape of GB1 does not show large energy barriers separating the different misfolded β-hairpins. This suggests that when one of the misfolded β-hairpins is formed, the system can reach

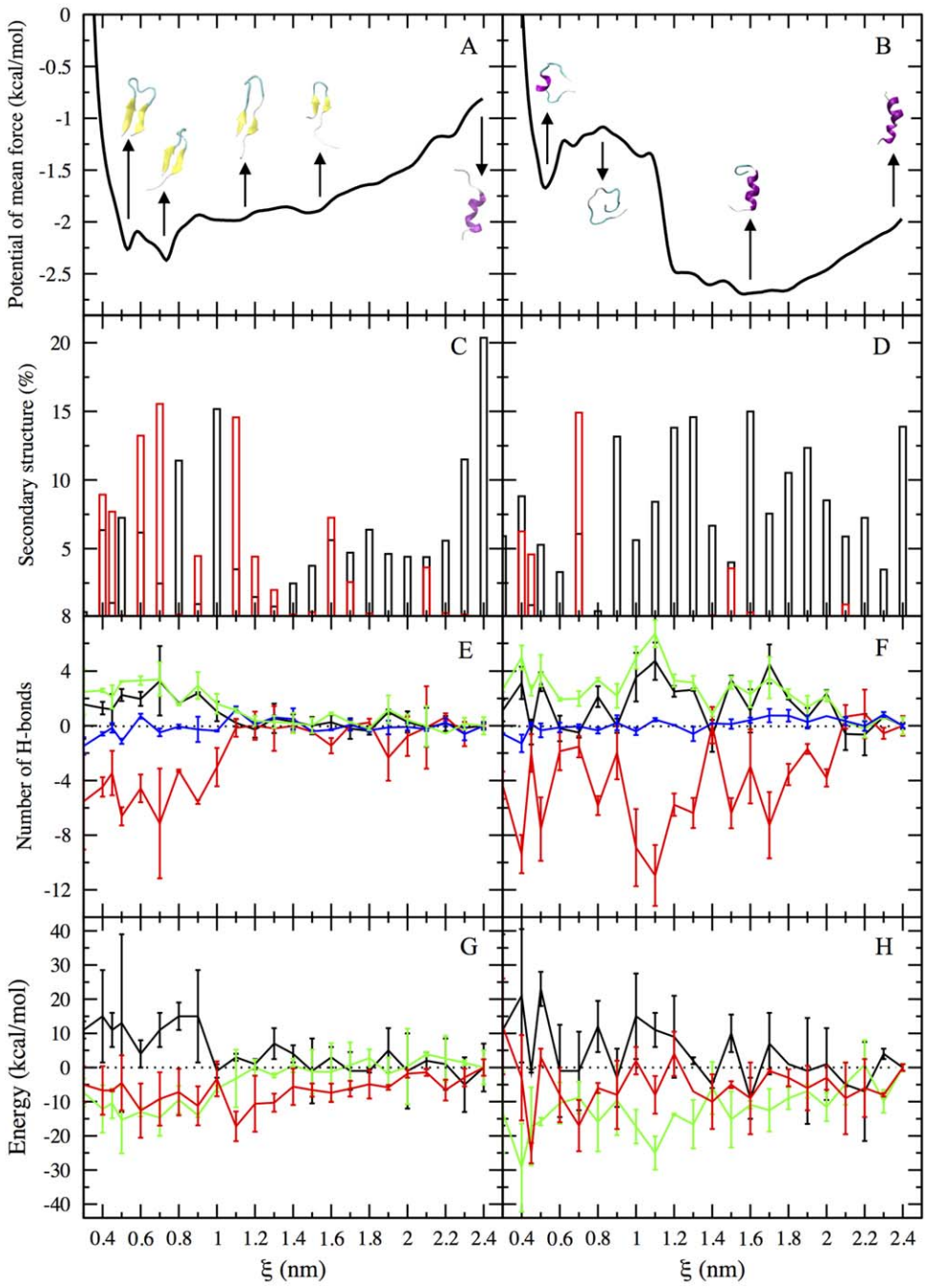

Figure 2

(**A, B**) PMF as a function of the end-to-end distance (ξ) for the GB1 peptide (A) and the E2 isoform (B). Representative conformations corresponding to the different energy minima and the free energy barriers for the GB1 peptide and the E2 isoform are shown in a cartoon representation. (**C, D**) Percent secondary structure as a function of ξ for GB1 (C) and the E2 isoform (B). Helical content is shown in black while the β-strand content is displayed in red. (**E, F**) Rescaled values for the peptide–peptide (black), peptide–water (red), water–water (green), and total (blue) hydrogen bonds as a function of ξ for GB1 (E) and the E2 isoform (F). (**G, H**) Rescaled values for the Coulomb (black), van der Waals (green), and total (red) energies as a function of ξ for GB1 (G) and the E2 isoform (H). Error bars represent the standard error of the mean from the two simulations.

the other hairpins and the native structure through a reptation-like mechanism.[47] In this mechanism, hydrogen bonds break and reform during the transition from the different misfolded structures to the native-like hairpin conformation [Fig. 3(B)]. Reptation mechanism has been reported previously[47] for GB1 although most computer simulations report β-hairpin formation initiated at the native turn.[45,52,70,71]

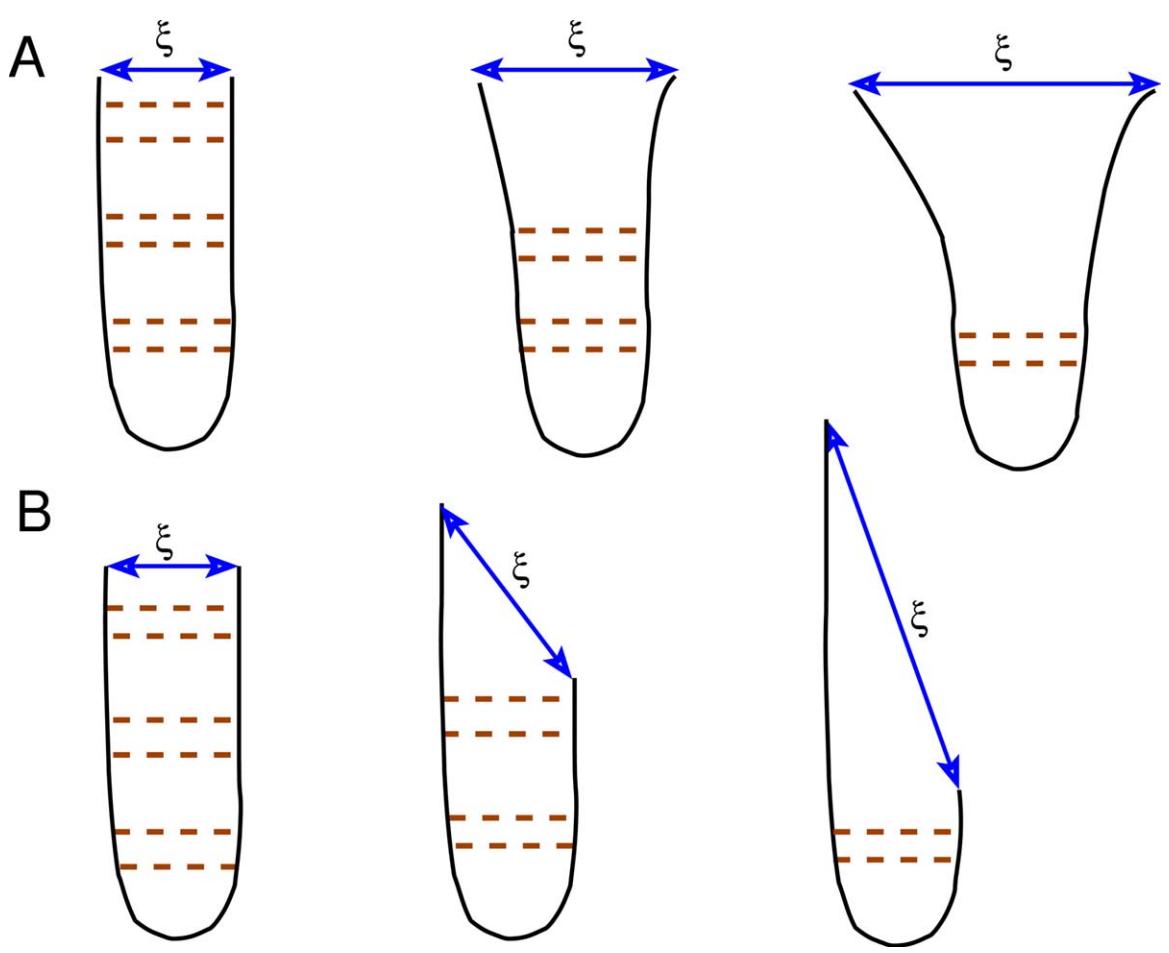

Figure 3

Schematic representation of the zipper-like (**A**) and roll-up (**B**) mechanisms for β-hairpin formation. [Color figure can be viewed in the online issue, which is available at wileyonlinelibrary.com.]

Misfolded β-hairpins could also emerge as the result of a roll-up mechanism proposed recently for Chignolin.[72] In this mechanism, one end of the peptide is kept rigid while the other rolls-up displacing the turn to the middle of the chain. The enhanced rigidity of one end with respect to the other is a key constituent for folding to proceed. Enemark *et al.*[72] showed that this rigidity is conferred by frequent interactions between aromatic residues at positions i and $i + 2$ which restrict main-chain movement. This could be the rationale for the presence of two aromatic residues at a short distance from each other at the rigid N-termini of GB1. The presence of aromatic residues at positions i and $i + 2$ is however not enough to guarantee a robust energy landscape favoring β-hairpins as demonstrated by the E2 isoform peptide. These aromatic residues have to be positioned close to the turn,[40,50–52] suggesting that the intrinsic propensity of residues 7–10 of GB1 to form turns is not enough to account for the native structure. It requires a reinforcement of hydrophobic interactions to be stabilized.

The misfolded β-hairpins observed in this study correspond to characteristic structures of equilibrium ensembles which have fixed end-to-end distances. Based on our simulations alone, it is, therefore, not possible to determine the sequential order of events that leads to correctly folded β-hairpin which is required to discriminate between reptation, zipper, and roll-up mechanisms. Nevertheless, our simulations predict that the ensemble of unfolded structures will be populated by misfolded β-hairpins. To assess if these structures are indeed observed in kinetic simulations, we performed a set of five unconstrained simulations of the GB1 peptide. Simulations were performed using starting conformations with end-to-end distances of 1.6 nm for a total of 300 ns. We identified misfolded conformations similar to those observed in the end-to-end restrained simulations (see Supporting Information Fig. S2), suggesting that misfolded β-hairpins observed in our simulations are not artifacts of the sampling methodology.

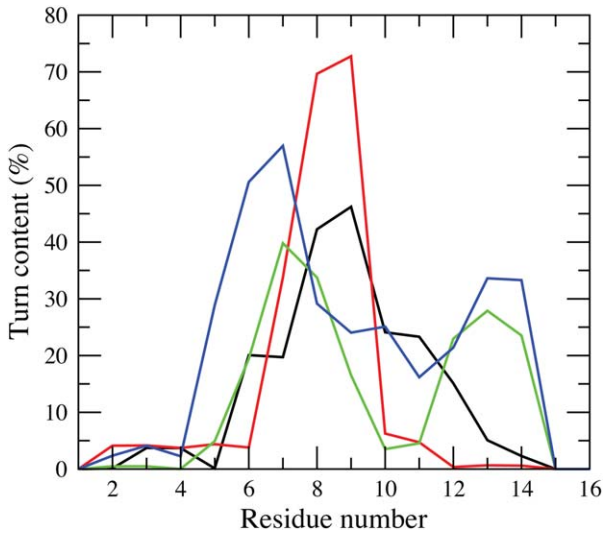

Figure 4

Average percent turn content as a function of the residue number for end-to-end distances of 0.4 (black), 0.7 (red), 1.2 (green), and 1.6 nm (blue) for the GB1 peptide. [Color figure can be viewed in the online issue, which is available at wileyonlinelibrary.com.]

Hydrogen bonds are not main interactions driving secondary structure formation

Figure 2(E,F) shows the peptide–peptide, peptide–water, water–water, and total hydrogen bonding calculated for GB1 (E) and the E2 isoform (F). For GB1, the number of peptide–peptide hydrogen bonds (black) increases at end-to-end distances corresponding to β-hairpin conformations. The number of water–water hydrogen bonds (green) shows a similar trend, suggesting that as the peptide forms intra-chain hydrogen bonds, the displaced water molecules are transferred to the bulk, resulting in a corresponding increase in the number of water–water hydrogen bonds. This is supported by the observation that the number of peptide–water hydrogen bonds (red) decreases as the peptide–peptide and water–water interactions increase. We note that the net number of hydrogen bonds (blue) does not change significantly for all values of ξ. This is in agreement with Schellman's[73] and Kauzmann's[74] hypotheses that hydrogen bonds in aqueous solution do not play an important role in protein folding.[75] Our results are also in agreement with previous simulations on *N*-methylacetamine[76] and homo-peptide dimers made of aliphatic side chains.[77] These simulations also reported negligible role of hydrogen bonding during secondary structure formation. Nevertheless, this is surprising because it contradicts most interpretations of the zipper mechanism for which hydrogen bonding is a key component in zipping the two strands together.

Hydrogen bonding trends for the E2 isoform are similar to that of the GB1 peptide. The number of peptide–peptide hydrogen bonds (black) is higher for the preferred α-helical conformations at intermediate end-to-end distances suggesting greater intra-peptide hydrogen bonding [Fig. 2(F)]. A corresponding increase in the water–water hydrogen bonding is observed at these end-to-end distances. The number of peptide–water interactions is lower for the regions where the peptide–peptide and water–water interactions are higher. The total number of hydrogen bonds (blue) does not show a significant change as a function of the end-to-end distance for the E2 isoform.

Coulomb and van der Waals energies contribute differently to the formation of secondary structures

Figure 2(G,H) shows the rescaled values (see Methods) of the average Coulomb (black), van der Waals (green), and total energies (red) as a function of the end-to-end distance for GB1 and the E2 isoform. Coulomb energies are large and unfavorable at small end-to-end distances (<1 nm) and these values decrease with increasing end-to-end distance. In contrast, van der Waals interactions contribute favorably to the formation of β-hairpin structures. The total energy is dominated by the behavior of van der Waals interactions and it is negative along the entire reaction coordinate for GB1. This is different from results from implicit water simulations which suggest that electrostatic interactions are main driving forces for folding of GB1.[78]

Energetic contributions for the E2 isoform are subjected to larger fluctuations. The average total energy for the E2 isoform is favorable along entire length of the reaction coordinate, similar to that observed for the GB1 peptide. Coulomb interactions are unfavorable for most of the end-to-end distances explored while van der Waals interactions are favorable over the entire range of end-to-end distances.

CONCLUSIONS

Transitions from α-helix or coil states to β-sheets are essential for the formation of fibrillar aggregates, observed in various disease states.[19,23,36,79,80] Here, we used the GB1 peptide and the E2 isoform as model peptides to study large conformational changes associated with the formation of β-hairpin and α-helical structures. Peptides were simulated over a range of end-to-end distances that explore both β-hairpin (∼0.4–0.7 nm) and α-helical (∼2.2–2.4 nm) conformations. We examined free energy landscapes of GB1 and the E2 isoform in explicit solvent. In agreement with previous studies[37,49] we show that β-hairpin is the minimum free energy conformation for GB1. In addition to the presence of helical conformations close to the C-termini,[49] the unfolded state of GB1 is also populated by misfolded β-hairpins

which differ from each other in the location of the β-turn. The existence of one of the misfolded β-hairpins was reported previously.[69] These observations suggest that the unfolded state of GB1 may not be as disordered as commonly thought. In contrast, the E2 isoform adopts predominantly α-helical conformations with a stable partially folded α-helix being the preferred free energy minimum.[40]

In a recent computer simulation, side chain interactions were shown to be a main force driving β-sheet formation of model peptides while hydrogen bonds were shown to play a minimal role in this process.[77] A limitation of this work was that peptides were kept elongated during the simulations. Here, we show that even when the backbone of the peptide is not restrained, the total number of hydrogen bonds does not change during the formation of the β-hairpin while the total electrostatic energy of the system becomes unfavorable, that is, it increases. Hydrogen bond energies in all-atom models are a result of electrostatic interactions between hydrogen donor and acceptor groups. This suggests that hydrogen bonding might not be a major driving force for the formation of secondary structures in GB1 and the E2 isoform. A possible role of hydrogen bonding might be to restrict the conformational space of proteins, penalizing structures for which the total number of hydrogen bonds is not optimized. Configurations where hydrogen bond donors or acceptors of the backbone are unsatisfied would have a large electrostatic energy and would therefore occur rarely. We hypothesize that restriction of the conformational space to configurations with optimized hydrogen bonding could be a key factor accounting for fibril formation.

From an enthalpic point of view, the formation of β-sheets in the GB1 peptide is characterized by favorable van der Waals interactions and unfavorable Coulomb energies. This implies that as far as Coulomb interactions are concerned, extended conformations with large peptide exposure to water are more favorable than β-hairpin conformations. In contrast, van der Waals interactions favor the more compact β-hairpin conformation. Although average values of the different energetic terms computed for the E2 isomer are subjected to large fluctuations in our simulations, they exhibit a similar trend: compact conformations have favorable van der Waals and unfavorable Coulomb energies.

Entropic energies ($-T\Delta S$) at different end-to-end distances for both systems studied here were not computed due to their prohibitive computational cost. However, we can speculate that they have two main contributions which are due to water molecules around non-polar residues, that is, shell water, and the backbone of the peptide. Shell water around non-polar residues have a high Gibbs free energy (low entropy) due to the reduced number of conformations they assume compared to bulk water. Thus, entropic energies due to shell water favor compact conformation with small end-to-end distances as these conformations have a smaller number of shell water. In contrast, the backbone of the peptide assumes a larger number of conformations in the unfolded state which is, therefore, favored by backbone entropy.

In summary, the energetic picture that emerges from this study is that Van der Waals and hydrophobic interactions drive the formation of β-hairpins in the GB1 peptide while Coulomb interactions and the entropy of the backbone oppose it. A similar picture also emerges for the E2 isomer. However, our simulations for the E2 isomer are subjected to large error bars.

The objective of this study was to explore the free energy landscape associated with the transition from β-hairpin to α-helical conformations. The end-to-end distance of the peptide was chosen as the reaction coordinate since (1) it distinguishes α-helices from β-hairpin conformations, and (2) it is suitable for umbrella sampling simulations. Although the end-to-end distance is an unnatural constraint, structures obtained in this study, for example, misfolded β-hairpin of GB1, are also observed in unconstrained simulations of GB1, indicating that conformations obtained from the constrained simulations are not artifacts. Further, this study can be extended to explore energy landscapes of naturally occurring chameleon peptides[81,82] that have an equal propensity to adopt both α-helix and β-strand conformations. This methodology can also be used effectively to characterize structural transitions from α-helix to β-sheet conformations observed in amyloid-β and other peptides involved in disease states.[19,23,36,79,80]

REFERENCES

1. Chiti F, Dobson CM. Protein misfolding, #functional lamyloid, and human disease. Annu Rev Biochem 2006;75:333–366.
2. Selkoe DJ. Folding proteins in fatal ways. Nature 2003;426:900–904.
3. Benzinger TL, Gregory DM, Burkoth TS, Miller-Auer H, Lynn DG, Botto RE, Meredith SC. Propagating structure of Alzheimer's β-amyloid (10-35) is parallel β-sheet with residues in exact register. Proc Natl Acad Sci USA 1998;95:13407–13412.
4. Lührs T, Ritter C, Adrian M, Riek-Loher D, Bohrmann B, Döbeli H, Schubert D, Riek R. 3D structure of Alzheimer's amyloid-β (1-42) fibrils. Proc Natl Acad Sci USA 2005;102:17342–17347.
5. Antzutkin ON, Balbach JJ, Leapman RD, Rizzo NW, Reed J, Tycko R. Multiple quantum solid-state NMR indicates a parallel, #not lantiparallel, organization of β-sheets in Alzheimer's β-amyloid fibrils. Proc Natl Acad Sci USA 2000;97:13045–13050.
6. Antzutkin ON, Leapman RD, Balbach JJ, Tycko R. Supramolecular structural constraints on Alzheimer's β-amyloid fibrils from electron microscopy and solid-state nuclear magnetic resonance. Biochemistry 2002;41:15436–15450.
7. Chen M, Margittai M, Chen J, Langen R. Investigation of alpha-synuclein fibril structure by site-directed spin labeling. J Biol Chem 2007;282:24970–24979.
8. Tycko R, Savtchenko R, Ostapchenko VG, Makarava N, Baskakov IV. The α-helical C-terminal domain of full-length recombinant PrP converts to an in-register parallel β-sheet structure in PrP fibrils: evidence from solid state nuclear magnetic resonance. Biochemistry 2010;49:9488–9497.

9. Shewmaker F, Wickner RB, Tycko R. Amyloid of the prion domain of Sup35p has an in-register parallel β-sheet structure. Proc Natl Acad Sci USA 2006;103:19754–19759.
10. Qiang W, Yau W-M, Luo Y, Mattson MP, Tycko R. Antiparallel β-sheet architecture in Iowa-mutant β-amyloid fibrils. Proc Natl Acad Sci USA 2012;109:4443–4448.
11. Lansbury PT, Costa PR, Griffiths JM, Simon EJ, Auger M, Halverson KJ, Kocisko DA, Hendsch ZS, Ashburn TT, Spencer RG. Structural model for the β-amyloid fibril based on interstrand alignment of an antiparallel-sheet comprising a C-terminal peptide. Nat Struct Mol Biol 1995;2:990–998.
12. Tycko R. Progress towards a molecular-level structural understanding of amyloid fibrils. Curr Opin Struct Biol 2004;14:96–103.
13. Sawaya MR, Sambashivan S, Nelson R, Ivanova MI, Sievers SA, Apostol MI, Thompson MJ, Balbirnie M, Wiltzius JJ, McFarlane HT. Atomic structures of amyloid cross-β spines reveal varied steric zippers. Nature 2007;447:453–457.
14. Makin OS, Atkins E, Sikorski P, Johansson J, Serpell LC. Molecular basis for amyloid fibril formation and stability. Proc Natl Acad Sci USA 2005;102:315–320.
15. Marshall KE, Serpell LC. Insights into the structure of amyloid fibrils. Open Biol J 2009;2:185–192.
16. Swietnicki W, Morillas M, Chen SG, Gambetti P, Surewicz WK. Aggregation and fibrillization of the recombinant human prion protein. huPrP90-231. Biochemistry 2000;39:424–431.
17. Morillas M, Vanik DL, Surewicz WK. On the mechanism of α-helix to β-sheet transition in the recombinant prion protein. Biochemistry 2001;40:6982–6987.
18. Pan K-M, Baldwin M, Nguyen J, Gasset M, Serban A, Groth D, Mehlhorn I, Huang Z, Fletterick RJ, Cohen FE. Conversion of alpha-helices into beta-sheets features in the formation of the scrapie prion proteins. Proc Natl Acad Sci USA 1993;90:10962–10966.
19. Barrow CJ, Yasuda A, Kenny P, Zagorski MG. Solution conformations and aggregational properties of synthetic amyloid β peptides of Alzheimer's disease: analysis of circular dichroism spectra. J Mol Biol 1992;225:1075–1093.
20. Olsen KA, Fesinmeyer RM, Stewart JM, Andersen NH. Hairpin folding rates reflect mutations within and remote from the turn region. Proc Natl Acad Sci USA 2005;102:15483–15487.
21. Fesinmeyer RM, Hudson FM, Andersen NH. Enhanced hairpin stability through loop design: the case of the protein G B1 domain hairpin. J Am Chem Soc 2004;126:7238–7243.
22. Booth DR, Sunde M, Bellotti V, Robinson CV, Hutchinson WL, Fraser PE, Hawkins PN, Dobson CM, Radford SE, Blake CC. Instability, unfolding and aggregation of human lysozyme variants underlying amyloid fibrillogenesis. Nature 1997;385:787–793.
23. Liu L, Cao Z. Turn-directed α-β conformational transition of α-syn12 peptide at different ph revealed by unbiased molecular dynamics simulations. Int J Mol Sci 2013;14:10896–10907.
24. Kelly JW. The environmental dependency of protein folding best explains prion and amyloid diseases. Proc Natl Acad Sci USA 1998; 95:930–932.
25. Otzen DE, Kristensen O, Oliveberg M. Designed protein tetramer zipped together with a hydrophobic Alzheimer homology: a structural clue to amyloid assembly. Proc Natl Acad Sci USA 2000;97: 9907–9912.
26. López de la Paz M, de Mori G, Serrano L, Colombo G. Sequence dependence of amyloid fibril formation: insights from molecular dynamics simulations. J Mol Biol 2005;349:583–596.
27. Gazit E. A possible role for π-stacking in the self-assembly of amyloid fibrils. FASEB J 2002;16:77–83.
28. Levy Y, Jortner J, Becker OM. Solvent effects on the energy landscapes and folding kinetics of polyalanine. Proc Natl Acad Sci USA 2001;98:2188–2193.
29. Dias CL, Karttunen M, Chan HS. Hydrophobic interactions in the formation of secondary structures in small peptides. Phys Rev E 2011;84:041931.
30. Dias CL. Unifying microscopic mechanism for pressure and cold denaturations of proteins. Phys Rev Lett 2012;109:048104.
31. Wei G, Shea JE. Effects of solvent on the structure of the Alzheimer amyloid-beta(25-35) peptide. Biophys J 2006;91:1638–1647.
32. Daidone I, Simona F, Roccatano D, Broglia RA, Tiana G, Colombo G, Di Nola A. Beta-hairpin conformation of fibrillogenic peptides: structure and alpha-beta transition mechanism revealed by molecular dynamics simulations. Proteins 2004;57:198–204.
33. Heller WT, Waring AJ, Lehrer RI, Huang HW. Multiple states of beta-sheet peptide protegrin in lipid bilayers. Biochemistry 1998;37: 17331–17338.
34. Chiti F, Calamai M, Taddei N, Stefani M, Ramponi G, Dobson CM. Studies of the aggregation of mutant proteins in vitro provide insights into the genetics of amyloid diseases. Proc Natl Acad Sci USA 2002;99 Suppl 4:16419–16426.
35. Ding F, Borreguero JM, Buldyrey SV, Stanley HE, Dokholyan NV. Mechanism for the α-helix to β-hairpin transition. Proteins 2003; 53:220–228.
36. Singh S, Chiu C-C, Reddy AS, de Pablo JJ. α-helix to β-hairpin transition of human amylin monomer. J Chem Phys 2013;138: 155101.
37. Garcia AE, Sanbonmatsu KY. Exploring the energy landscape of a beta hairpin in explicit solvent. Proteins 2001;42:345–354.
38. Zagrovic B, Snow CD, Shirts MR, Pande VS. Simulation of folding of a small alpha-helical protein in atomistic detail using worldwide-distributed computing. J Mol Biol 2002;323:927–937.
39. Ma B, Nussinov R. Molecular dynamics simulations of a beta-hairpin fragment of protein G: balance between side-chain and backbone forces. J Mol Biol 2000;296:1091–1104.
40. Ma B, Nussinov R. Energy landscape and dynamics of the β-hairpin G peptide and its isomers: topology and sequences. Prot Sci 2003; 12:1882–1893.
41. Andrec M, Felts AK, Gallicchio E, Levy RM. Protein folding pathways from replica exchange simulations and a kinetic network model. Proc Natl Acad Sci USA 2005;102:6801–6806.
42. Weinstock DS, Narayanan C, Felts AK, Andrec M, Levy RM, Wu KP, Baum J. Distinguishing among structural ensembles of the GB1 peptide: REMD simulations and NMR experiments. J Am Chem Soc 2007;129:4858–4859.
43. Best RB, Mittal J. Balance between α and β structures in ab initio protein folding. J Phys Chem B 2010;114:8790–8798.
44. Roccatano D, Amadei A, Nola AD, Berendsen HJ. A molecular dynamics study of the 41-56 β-hairpin from B1 domain of protein G. Prot Sci 1999;8:2130–2143.
45. Pande VS, Rokhsar DS. Molecular dynamics simulations of unfolding and refolding of a beta-hairpin fragment of protein G. Proc Natl Acad Sci USA 1999;96:9062–9067.
46. Zhou R, Berne BJ, Germain R. The free energy landscape for β-hairpin folding in explicit water. Proc Natl Acad Sci USA 2001;98: 14931–14936.
47. Wei G, Mousseau N, Derreumaux P. Complex folding pathways in a simple β-hairpin. Proteins 2004;56:464–474.
48. Best RB, Mittal J. Microscopic events in β-hairpin folding from alternative unfolded ensembles. Proc Natl Acad Sci USA 2011;108: 11087–11092.
49. Gallicchio E, Andrec M, Felts AK, Levy RM. Temperature weighted histogram analysis method, #replica lexchange, and transition paths. J Phys Chem B 2005;109:6722–6731.
50. Espinosa JF, Muñoz V, Gellman SH. Interplay between hydrophobic cluster and loop propensity in β-hairpin formation. J Mol Biol 2001;306:397–402.
51. Klimov D, Thirumalai D. Mechanisms and kinetics of β-hairpin formation. Proc Natl Acad Sci USA 2000;97:2544–2549.
52. Muñoz V, Henry ER, Hofrichter J, Eaton WA. A statistical mechanical model for β-hairpin kinetics. Proc Natl Acad Sci USA 1998;95: 5872–5879.

53. Juraszek J, Bolhuis PG. Effects of a mutation on the folding mechanism of a beta-hairpin. J Phys Chem B 2009;113:16184–16196.
54. Torrie GM, Valleau JP. Nonphysical sampling distributions in Monte Carlo free-energy estimation: umbrella sampling. J Comput Phys 1977;23:187–199.
55. Hess B, Kutzner C, van der Spoel D, Lindahl E. GROMACS 4: algorithms for highly efficient, load-balanced, and scalable molecular simulation. J Chem Theory Comput 2008;4:435–447.
56. Sorin EJ, Pande VS. Exploring the helix-coil transition via all-atom equilibrium ensemble simulations. Biophys J 2005;88:2472–2493.
57. Best RB, Hummer G. Optimized molecular dynamics force fields applied to the helix-coil transition of polypeptides. J Phys Chem B 2009;113:9004–9015.
58. Lindorff-Larsen K, Piana S, Palmo K, Maragakis P, Klepeis JL, Dror RO, Shaw DE. Improved side-chain torsion potentials for the Amber ff99SB protein force field. Proteins 2010;78:1950–1958.
59. Jorgensen WL, Chandrasekhar J, Madura JD, Impey RW, Klein ML. Comparison of simple potential functions for simulating liquid water. J Chem Phys 1983;79:926–935.
60. Bussi G, Donadio D, Parrinello M. Canonical sampling through velocity rescaling. J Chem Phys 2007;126:014101–014101.
61. Parrinello M, Rahman A. Polymorphic transitions in single crystals: a new molecular dynamics method. J Appl Phys 1981;52:7182.
62. Kumar S, Rosenberg JM, Bouzida D, Swendsen RH, Kollman PA. The weighted histogram analysis method for free energy calculations on biomolecules. I. The method. J Comput Chem 1992;13:1011–1021.
63. Hub JS, de Groot BL, van der Spoel D. g_wham—a free weighted histogram analysis implementation including robust error and autocorrelation estimates. J Chem Theory Comput 2010;6:3713–3720.
64. Kabsch W, Sander C. Dictionary of protein secondary structure: pattern recognition of hydrogen-bonded and geometrical features. Biopolymers 1983;22:2577–2637.
65. Daura X, Gademann K, Jaun B, Seebach D, van Gunsteren WF, Mark AE. Peptide folding: when simulation meets experiment. Angew Chem Int Ed 1999;38:236–240.
66. Chetty PS, Mayne L, Lund-Katz S, Stranz D, Englander SW, Phillips MC. Helical structure and stability in human apolipoprotein AI by hydrogen exchange and mass spectrometry. Proc Natl Acad Sci USA 2009;106:19005–19010.
67. Daggett V, Levitt M. Molecular dynamics simulations of helix denaturation. J Mol Biol 1992;223:1121–1138.
68. Hansmann UHE, Okamoto Y. Finite-size scaling of helix-coil transitions in poly-alamine studied by multicanonical simulations. J Chem Phys 1999;110:1267–1276.
69. Bonomi M, Branduardi D, Gervasio FL, Parrinello M. The unfolded ensemble and folding mechanism of the C-terminal GB1 β-hairpin. J Am Chem Soc 2008;130:13938–13944.
70. Yoda T, Sugita Y, Okamoto Y. Cooperative folding mechanism of a β-hairpin peptide studied by a multicanonical replica-exchange molecular dynamics simulation. Proteins 2007;66:846–859.
71. Zhou R, Berne BJ, Germain R. The free energy landscape for beta hairpin folding in explicit water. Proc Natl Acad Sci USA 2001;98:14931–14936.
72. Enemark S, Kurniawan NA, Rajagopalan R. β-hairpin forms by rolling up from C-terminal: topological guidance of early folding dynamics. Sci Rep 2012;2:649.
73. Schellman JA. The stability of hydrogen-bonded peptide structures in aqueous solution. Comptes rendus des travaux du Laboratoire Carlsberg. Série chimique 1955;29.
74. Kauzmann W. Some factors in the interpretation of protein denaturation. Adv Protein Chem 1959;14:1–63.
75. Baldwin RL. In search of the energetic role of peptide hydrogen bonds. J Biol Chem 2003;278:17581–17588.
76. Jorgensen WL. Interactions between amides in solution and the thermodynamics of weak binding. J Am Chem Soc 1989;111:3770–3771.
77. Narayanan C, Dias CL. Hydrophobic interactions and hydrogen bonds in β-sheet formation. J Chem Phys 2013;139.
78. Evans DA, Wales DJ. Folding of the GB1 hairpin peptide from discrete path sampling. J Chem Phys 2004;121:1080–1090.
79. Morillas M, Vanik DL, Surewicz WK. On the mechanism of α-helix to β-sheet transition in the recombinant prion protein. Biochemistry 2001;40:6982–6987.
80. Xu Y, Shen J, Luo X, Zhu W, Chen K, Ma J, Jiang H. Conformational transition of amyloid β-peptide. Proc Natl Acad Sci USA 2005;102:5403–5407.
81. Zhou X, Alber F, Folkers G, Gonnet GH, Chelvanayagam G. An analysis of the helix-to-strand transition between peptides with identical sequence. Proteins 2000;41:248–256.
82. Mou CY, Lin CY, Chen NY. Folding a protein with equal probability of being helix or hairpin. Biophys J 2012;103:99–108.